On the understanding of the remarkable activity of template-containing mesoporous molecular sieves in the transesterification of rapeseed oil with ethanol

Demian Patrick Fabiano [a,b], Berna Hamad [a], Dilson Cardoso [c], Nadine Essayem [a,*]

[a] Institut de Recherche sur la Catalyse et l'Environnement de Lyon, IRCELYON, Université Lyon 1, CNRS, UMR5256, Villeurbanne, France
[b] Chemical Engineering, Federal University of São João del-Rei, Rodovia MG 443, km 7, CEP 36420-000, Ouro Branco, MG, Brazil
[c] Chemical Engineering Department, Federal University of São Carlos, Rodovia Washington Luís, km 235, CEP 13565-905 São Carlos, SP, Brazil

ARTICLE INFO

ABSTRACT

Ordered mesoporous molecular sieves of the M41S family, containing their organic template, were evaluated as-synthesized in a basic catalyzed reaction, the transesterification of rapeseed oil with ethanol. These materials [CTA]Si–MCM-48, [CTA]Si–MCM-50, [CTA]Si–MCM-41 (CTA stands for cetyltrimethylammonium cation), which still possess their organic template occluded in the silica pores, were characterized by calorimetry of CO_2 adsorption. These hybrid catalysts present weak basic sites, with low differential heat of CO_2 adsorption between 70 and 90 kJ mol^{-1}; however, the adsorption phenomena were disclosed to be totally reversible at 30 °C. Surprisingly, these hybrid catalysts were shown to be remarkable catalysts for the transesterification of rapeseed oil with ethanol in mild temperature conditions, 79 °C: a total oil conversion was achieved in 1 h with the [CTA]Si–MCM-48, while in equivalent conditions, one of the most efficient mineral solid base, ZrOCs, gave only a conversion of 65%. ZrOCs is considered as a solid base of higher strength, characterized by the heat of CO_2 adsorption of 130 kJ mol^{-1}; interestingly, the CO_2 adsorption is totally irreversible at 30 °C. The most active material in the hybrid molecular sieves series, [CTA]Si–MCM-48, possesses active sites in intermediate position between physisorption and chemisorption in regard to CO_2 adsorption. This solid is characterized by the presence of the most energetic centers within the hybrid catalysts series with the heat of CO_2 adsorption of 90 kJ mol^{-1} combined with a complete reversibility of the CO_2 adsorption.

1. Introduction

Transesterification of vegetable oils to produce biodiesel can be catalyzed by acid or basic sites, with homogeneous or heterogeneous catalysts. NaOH and KOH are the conventional catalysts for this reaction, because of their efficiency and low cost [1]. However, the use of these homogeneous basic catalysts in the transesterification of vegetable oils can produce soaps or emulsions, which are hardly removed [2]. Moreover, when the transesterification occurs in homogeneous phase, the catalyst removal is difficult and the final products separation is expensive due to the need of neutralization stages and biodiesel purification. On the opposite, when a heterogeneous catalyst is used, the saponification reaction is avoided. Substitution of soluble bases by a solid catalyst presents the additional advantage of production of glycerol of high purity without purification steps [3]. In this field, there is no doubt about the real interest of developing a solid catalyst, which would be as active as the homogeneous alkali bases in mild conditions. The important research effort in that direction is attested by the increasing number of publications in this field [3].

In the 1990s, the scientists from Mobil Company have discovered a new family of ordered mesoporous molecular sieves, designated as M41S. These materials are synthesized under hydrothermal conditions from silicate/alumino-silicate gels containing organic surfactant molecules [4]. They have a pore diameter ranging from 2 to 50 nm and a surface area in the range of 1000 m^2 g^{-1} [5,6]. These new materials were at the origin of the development of novel catalysts with enlarged active area, an important characteristic for the improvement of current industrial processes [7].

Usually, after the synthesis, these materials are calcined to remove the surfactant that is occluded in the mesopores. These materials were made only of silica walls, and they do not present marked catalytic properties. Usually, to develop some basic proprieties in the calcined materials, several techniques have been used: (i) the functionalization of the molecular sieve surface with compounds containing terminal amines. The anchoring points are the silanol groups obtained by calcination [8–10] and (ii) the dispersion of alkali metal oxides on the molecular sieve surface [8]. Usually, cesium acetate was used for the impregnation of the calcined MCM-41, followed by calcination at 450 °C aimed [11].

However, Kubota et al. [12,13] reported for the first time that the as-synthesized [CTA]Si–MCM-41 molecular sieve possesses active basic sites. These authors used this material in condensation

reactions when it still contained the organic structuring directing agent, the cetyltrimethylammonium cation (CTA^+). They suggested that the basic sites are the siloxi anions ($\equiv SiO^-$), interacting with the CTA^+ cations. Martins et al. [14] by using ^{29}Si MAS NMR and O1s XPS have shown that the active sites are indeed the basic siloxi anions ($\equiv SiO^-$) in the composite material and, as the mesopores are occluded, the reaction only occurred at the pore mouth [12–14].

Another study of Martins and Cardoso [15] has demonstrated that in a series of siliceous mesoporous molecular sieve [C_nTA]Si–MCM-41, synthesized with different surfactant chain lengths ($10 \leqslant n \leqslant 16$), the most voluminous cation ($C_{16}TA^+$) ensured the higher catalytic activity in the Knoevenagel condensation. The better activity of that material was correlated with the high-order degree of the synthesized material and with the largest amount of cations present on its surface.

Oliveira et al. [16] tested the as-synthesized molecular sieves as basic catalysts for Knoevenagel condensation, including the M41S mesoporous silica. They have observed that catalytic behavior was mainly dependent on the amount of framework silicon and they concluded that siloxi anions ($\equiv SiO^-$) should be the basic active sites. XPS measurements of these hybrid organic–inorganic catalysts have shown that the O1s binding energy is influenced by the presence of the organic template, leading to the conclusion that they are interacting with the framework oxygen, most likely balancing the framework anions.

Due to the high activity of the M41S catalysts in basic catalyzed reactions such as the Knoevenagel condensation, in the present work, we have evaluated the performances of these catalysts in the transesterification of rapeseed oil with ethanol at 79 °C. The organization and the textural properties of the as-synthesized materials were characterized by XRD, TGA, and nitrogen physisorption. The catalyst basicity was measured by CO_2 adsorption monitored by calorimetry and also by gravimetry. Finally, the basicity and the catalytic performances of the basic hybrid materials were compared to those of a more conventional solid base, zirconia promoted with Cs, which is a strong solid base showing a high catalytic activity transesterification [17].

2. Experimental

2.1. Synthesis of hybrid organic–inorganic molecular sieves and ZrOCs

2.1.1. [CTA]Si–MCM-41
The [CTA]Si–MCM-41 mesoporous molecular sieve was synthesized according to the methodology reported by Cheng et al. [18]. Samples were prepared from silica (Aerosil 380, Degussa), cetyltrimethylammonium bromide (CTABr, Acros organic) and tetramethylammonium hydroxide (TMAOH, Fluka). The composition of the reaction medium was 1 SiO_2:0.27 CTABr:0.19 TMAOH:40 H_2O. In 141.26 g of deionized water, 6.91 g of TMAOH·5H_2O and 19.76 g of CTABr were diluted. Then, the mixture was kept under stirring at 40 °C until a clear solution was achieved. After cooling the solution to room temperature, 12.06 g of silica Aerosil was added. The sample was aged for 24 h before the thermal treatment, which was carried out at 150 °C for 2 days. Finally, the sample was filtered, washed several times with deionized water up to pH $\sim$ 7, and dried at 60 °C for 24 h.

2.1.2. [CTA]Si–MCM-48
The [CTA]Si–MCM-48 mesoporous molecular sieve was synthesized according to Doyle et al. [19] procedure as follows: 26.7 g of cetyltrimethylammonium bromide was dispersed in 243.0 g of deionized water and 2.7 g of sodium hydroxide at 40 °C. To this solution, 27.6 g TEOS (tetraethylorthosilicate 98%, Acros Organic)

was added and the gel mixture was aged for 60 min at room temperature. The gel, having a molar composition of 1 SiO_2:0.55 CTABr:0.5 Na_2O:101.4 H_2O, was then treated at 100 °C for 48 h. After the hydrothermal treatment, the sample was filtered, washed successively with deionized water up to pH $\sim$ 7, and dried at 60 °C for 24 h.

2.1.3. [CTA]Si–MCM-50
The [CTA]Si–MCM-50 was prepared following the same procedure described for Si–MCM-48 synthesis [20]; however, hydrothermal treatment was carried out at 150 °C for 48 h.

2.1.4. ZrOCs
ZrOCs catalysts were prepared by cationic exchange of zirconium hydroxide with cesium carbonate, in basic conditions [17]. First, zirconium hydroxide was precipitated at pH 10 starting from $ZrOCl_2·8H_2O$. The exchange with Cs^+ was carried out as follows: 0.003 mol of Cs_2CO_3 was dissolved in 16 ml of water (pH 11); then, 1 g of zirconium hydroxide was added and mixed for 15 min. The exchanged solid was removed by filtration, dried at 110 °C, and calcined at 550 °C. Then, the calcined ZrOCs was washed two times in refluxed ethanol to remove the weakly bonded Cs species [17].

2.2. Characterizations

2.2.1. X-ray diffraction (XRD)
For the samples M41S, small-angle X-ray diffraction patterns was made within the interval $1 < 2\theta < 10°$. They were recorded with a Rigaku Multiflex diffractometer with the Cu Kα (40 kV, 40 mA) radiation. For the ZrOCs sample, the X-ray diffraction pattern was made within the interval $3 < 2\theta < 80°$.

2.2.2. Nitrogen physisorption
Nitrogen adsorption/desorption isotherms were recorded at liquid nitrogen temperature with an equipment supplied by Micromeritics (ASAP 2020). Before the analysis, the as-synthesized molecular sieves samples were vacuum treated at 120 °C for 2 h. Surface areas were estimated through BET equation using $p/p_0 \leqslant 0.3$ [21].

2.2.3. Thermogravimetric measurements
The quantification of the organic template present in silicate samples was performed using a thermogravimetric (Therma Analyst 2100) equipment. About 10 mg of the sample was placed in a platinum holder and heated from room temperature to 1000 °C, at a heating rate of 10 °C min^{-1} and under O_2 flow of 40 mL min^{-1}. The amount of cation CTA^+ per gram of SiO_2, present in the as-synthesized samples, was calculated considering the mass loss at temperatures ranging from 120 °C to 390 °C.

TG experiments were also performed in order to quantify the total capacity of CO_2 adsorption for the various catalysts. Fifteen milligrams of the basic hybrid samples was treated at 30 °C under vacuum for one night and equilibrated at the same temperature in an Ar flow. After this pre-treatment, the Ar flow was replaced by a mixture of CO_2 (1%) diluted in Ar (40 cm^3 min^{-1}) and left for 1 h. Thereafter, the gas flow was replaced by the flow of pure Ar to remove the reversible CO_2 uptake. For the mass differences before and after the contact with CO_2 and subsequent Ar flushing, the irreversible amount of adsorbed CO_2 was deduced.

2.2.4. Microcalorimetry studies of CO_2 adsorption
The basic properties were measured by CO_2 adsorption at 30 °C, using a TianCalvet calorimeter coupled with a volumetric equipment. The samples of hybrid materials (0.1 g) were first evacuated at 30 °C for 24 h under secondary vacuum while the ZrOCs was treated at 400 °C for 2 h (ramp 1 °C min^{-1}) under secondary

vacuum. After the pre-treatment, the samples were placed into the calorimeter up to the stabilization of the temperature (one night), then contacted with small doses of gas up to equilibrium and the differential enthalpy of adsorption was recorded together with the amount of adsorbed CO_2. After the first CO_2 isotherm (total CO_2 adsorption), the samples were vacuum treated at 30 °C for 10 h before performing the second CO_2 isotherm (reversible CO_2 adsorption).

2.3. Catalytic tests

The catalytic performances were evaluated in vegetable oil ethanolysis under the following standard conditions: the temperature of reaction was equal to 79 °C (ebullition temperature of the ethanol) and reaction was stopped after 5 h. Anhydrous Ethanol (Aldrich) and rapeseed oil (commercial) were used with a alcohol/triglyceride molar ratio of 18 and 2.5 wt.% of catalyst was used.

The transesterification reaction was carried out under inert atmosphere in a *Parr* autoclave, equipped with a Pyrex insert, a mechanic stirrer and a temperature controller.

Before the transesterification reaction, the ZrOCs sample was pre-treated at 400 °C under vacuum in order to remove part of the carbonate species and the hydration water, a parameter known to modify the basic strength. However, it is clear that this treatment is not efficient to remove the most stable carbonate species [17]. The hybrid catalysts were used without pre-treatment.

The reaction was stopped using a bath of a water/ice mixture for a rapid cooling of the reaction mixture. The catalyst was separated by filtration. For the GC analysis, the reaction medium was mixed with THF (tetrahydrofuran) in order to obtain a homogeneous phase.

The GC analysis was carried out using a capillary column purchased from Varian, CP 9048 (length: 30 m, diameter: 0.32 mm, thickness of the stationary phase: 0.1 mm). This column allows the separation of triglycerides, diglycerides, monoglycerides, and fatty methyl and ethyl esters. Helium was used as carrier gas. The injector and detector (FID) temperatures were, respectively, 280 and 340 °C. The split ratio was fixed at 100. The oven temperature program was as follows: start at 80 °C (1 min), ramp at 5 °C/min to 300 °C, then ramp at 25 °C/min to 380 °C. The samples were prepared for the analysis in order to get 10 wt.% of fatty products in THF [22]. Five milliliters of sample was injected into the column.

3. Results and discussion

3.1. Synthesis of hybrid organic–inorganic molecular sieves and ZrOCs

Fig. 1 shows the XRD patterns and the nitrogen physisorption isotherms of the catalysts. The XRD patterns show that the hybrids mesoporous materials of M41S family were very well organized. The as-synthesized [CTA]Si–MCM-41 showed typical low-angle XRD patterns, exhibiting four distinctive reflections, corresponding to the reflection planes (1 0 0), (1 1 0), (2 0 0), and (2 1 0) [4,6]. The [CTA]Si–MCM-48 exhibited eight XRD diffraction peaks at (2 1 1), (2 2 0), (3 2 1), (4 0 0), (4 2 0), (3 3 2), (4 2 2), and (4 3 1), which can be indexed to the Ia3d cubic structure [6]. The [CTA]Si– MCM-50 exhibited an intense diffraction peak (1 0 0), a second one of lower intensity (2 0 0), and a third one of low intensity (3 0 0); they are characteristic of this lamellar mesoporous silica material [6]. The nitrogen physisorption isotherms of the hybrids materials (Fig. 1) show that the materials present a low porosity and reduced superficial areas (Table 1), because their pores are still occluded by the template.

ZrOCs obtained after calcination at 550 °C is poorly crystalline, but only the diffraction peaks of the tetragonal zirconia phase are

detected [17]. The BET surface area of this material equals 71 m² g⁻¹, and the calcined solid is mainly mesoporous.

3.2. CO_2 adsorption monitored by microcalorimetry

The basic properties of the catalysts were determined by CO_2 adsorption at 30 °C monitored by microcalorimetry. After the completion of the first CO_2 adsorption isotherms (total adsorption), the catalysts were submitted to a vacuum treatment for 10 h at 30 °C aimed to remove the weakly bonded CO_2 molecule, before a second CO_2 adsorption isotherms (reversible adsorption) in order to characterize the reversibility of the adsorption. Note that for the most usual basic catalysts, the reversible CO_2 adsorption isotherm is of reduced extent.

Fig. 2 presents the evolution of the differential heat of CO_2 adsorption with the CO_2 coverage. The calorimetric curve of ZrOCs, recorded during the first CO_2 adsorption isotherm, presents few strong sites with differential heat of CO_2 adsorption higher than 130 kJ mol⁻¹ and an extended plateau near 120 kJ mol⁻¹ accounting for the presence of a high density of basic sites of homogeneous high strength. The total amount of basic sites, deduced from this first adsorption experiment, reached 375 μmol g⁻¹. By contrast, the calorimetric curve recorded during the second adsorption isotherm (reversible adsorption) presented initially few sites with lower differential heat of CO_2 adsorption (80 kJ mol⁻¹) and a fast saturation of the available sites.

Our interpretation is that during the first adsorption isotherm, most of the basic sites of ZrOCs were irreversibly saturated by CO_2 molecules, characterized by high enthalpies of CO_2 adsorption, as expected for a CO_2 chemisorption. Accordingly, the vacuum treatment applied to remove the weakly bonded CO_2 molecules (the reversible CO_2 uptake) remained of limited effect as shown by the second calorimetric curve recorded during to the reversible CO_2 isotherm.

Interestingly, in contrast to the ZrOCs oxide, the [CTA]Si–MCM-50 hybrid material presents a quite distinct behavior. The total and the reversible CO_2 adsorption isotherms are exactly similar (not shown) and accordingly the corresponding calorimetric curves are almost the same (see Fig. 2). The calorimetric curves showed initial differential heats of CO_2 adsorption close to 90 kJ mol⁻¹ and a continuous decrease in the enthalpy with the CO_2 coverage down to 50 kJ mol⁻¹, characterizing the presence of a few amount of weak basic sites (90 kJ mol⁻¹) completed by an heterogeneous distribution of less energetic sites. The low heat of CO_2 adsorption associated with the total reversibility of the CO_2 adsorption would rather be described in terms of physisorption rather than chemisorption. Another important observation is that the amount of CO_2 adsorbed on the [CTA]Si–MCM-50 sample is practically the same as the amount of sites probed on ZrOCs (375 μmol g⁻¹), which would indicate that the amount of potential active sites in the two materials is very close. Note that for the hybrid materials, the measured CO_2 capacity is unexpected and exceeds the monolayer coverage accounting for a possible CO_2 penetration into the templated mesopores mouths.

Therefore, one can conclude that the amounts of sites probed by CO_2 on the two types of materials are close; however, ZrOCs presents strong basic sites of homogeneous strength which irreversibly adsorbed CO_2 at 30 °C, whereas the [CTA]Si–MCM-50 presents sites of weaker strength and heterogeneous distribution characterized by a complete reversibility in regard to the CO_2 adsorption at 30 °C.

A Behavior similar to that presented by the [CTA]Si–MCM-50 sample is observed on the other materials belonging to the M41S family (Fig. 3). The differential heat of CO_2 adsorption measured for low CO_2 coverage on [CTA]Si–MCM-48 is close to that measured on [CTA]Si–MCM-50, 90 kJ mol⁻¹; then, it declines with the CO_2
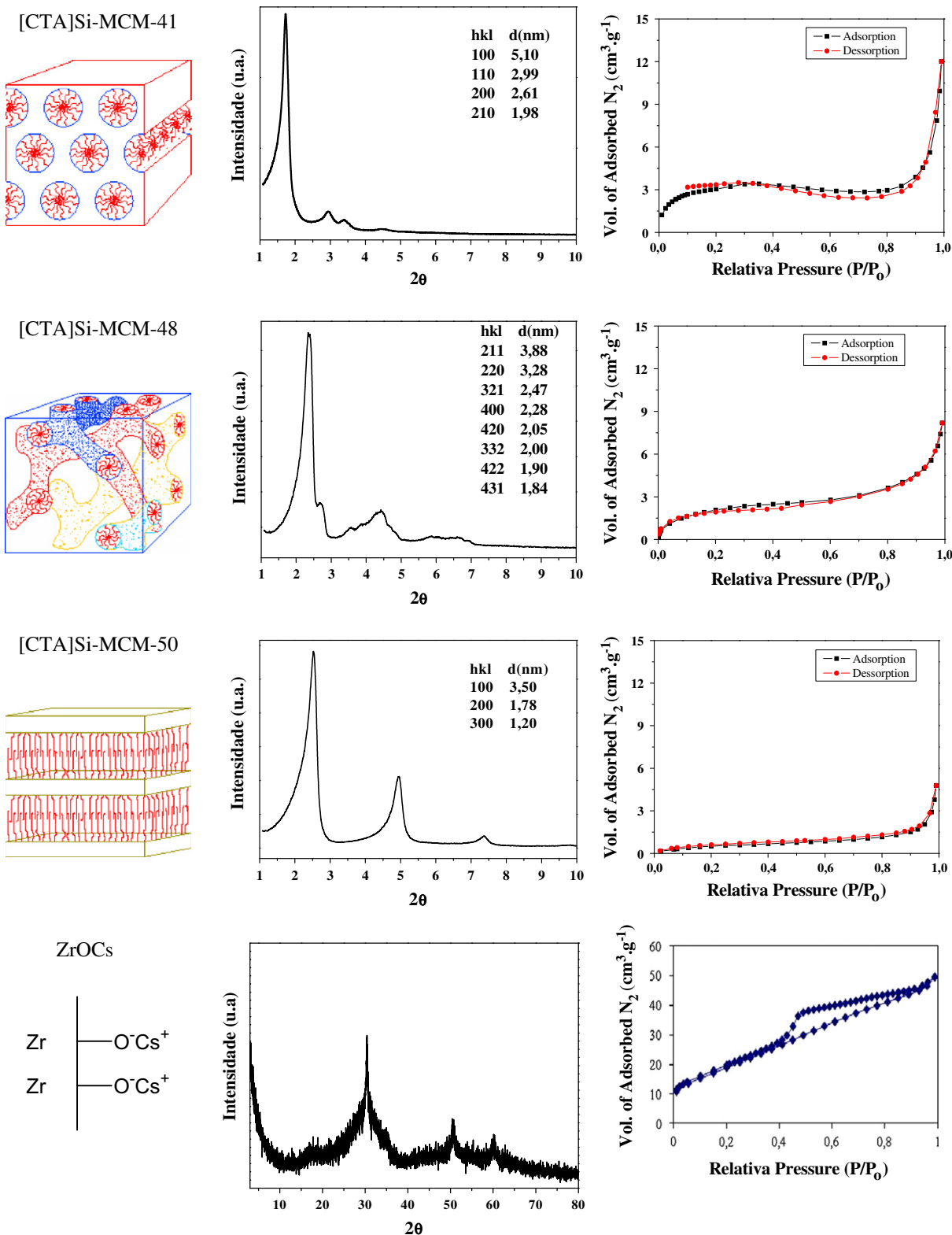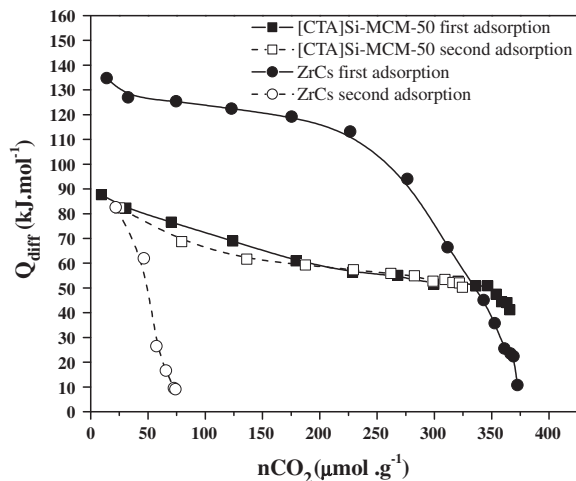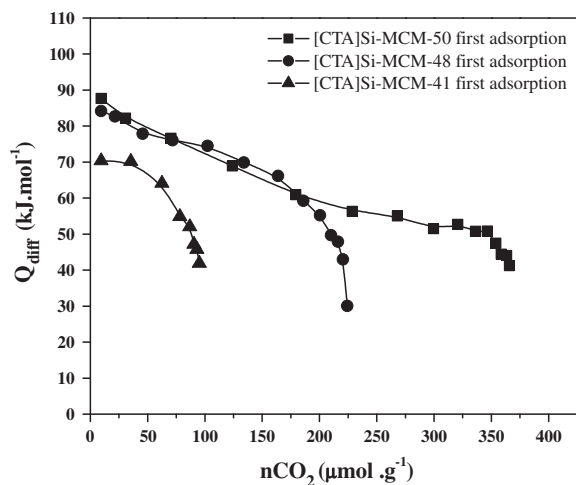
[CTA]Si-MCM-41

hkl	d(nm)
100	5,10
110	2,99
200	2,61
210	1,98

[CTA]Si-MCM-48

hkl	d(nm)
211	3,88
220	3,28
321	2,47
400	2,28
420	2,05
332	2,00
422	1,90
431	1,84

[CTA]Si-MCM-50

hkl	d(nm)
100	3,50
200	1,78
300	1,20

ZrOCs

Zr —— O⁻Cs⁺

Zr —— O⁻Cs⁺

Fig. 1. X-ray diffraction patterns and nitrogen physisorption isotherms.

coverage down to values of 30 kJ mol⁻¹. These two materials are synthesized from the same synthesis gel; however, the geometry of each material is different: the [CTA]Si–MCM-48 possesses a cubic geometry with tortuous pores in a three-dimensional system, and the [CTA]Si–MCM-50 has a lamellar geometry with pores in a two-dimensional system, as presented in the Fig. 1.

From the thermogravimetric analysis, it was possible to estimate the surfactant amount present in each material (Table 1). The cation/silica molar ratio equal 0.28 for the [CTA]Si–MCM-50 and for the [CTA]Si–MCM-48. One can observe that the surfactant amount in the two materials is the same, and the behavior in regard to CO_2 adsorption is similar with regard to the differential
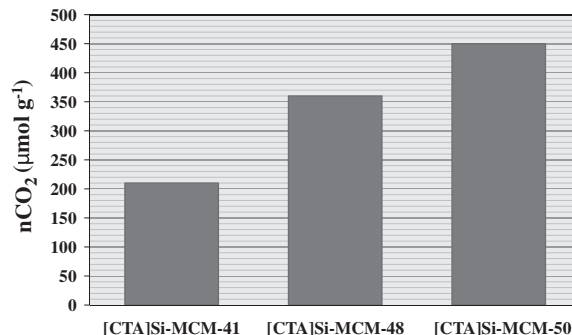
Table 1
Catalysts textural features.

Material	Molar ratio CTA/silica	$A_{0.3}$[a] ($m^2\,g^{-1}$)	V_p[b] ($cm^3\,g^{-1}$) $\times 10^2$
[CTA]Si–MCM-41	0.14	10.59	1.54
[CTA]Si–MCM-48	0.28	7.61	1.14
[CTA]Si–MCM-50	0.28	2.00	0.58
ZrOCs	–	71.00	–

[a] Surface area estimated from BET equation using $p/p_0 \leqslant 0.3$.
[b] Porous volume.

Fig. 2. Differential heat of CO_2 adsorption as a function of CO_2 coverage.

Fig. 3. Differential heat of CO_2 adsorption as a function of CO_2 coverage.

Fig. 4. CO_2 adsorption on the hybrids materials measured by gravimetry.

of CO_2 adsorption of 70 kJ mol^{-1} and a subsequent continuous decrease in the differential heat of adsorption with the CO_2 coverage. Upon CO_2 saturation, the total amount of sites probed by CO_2 achieved only 100 μmol g^{-1}. This reduced ability in CO_2 adsorption could be ascribed to its lower amount of surfactant, compared to the other materials and its one-dimensional pores system.

Another method was applied to check the total amount of CO_2 adsorption in dynamic conditions. Fig. 4 shows the total amount of CO_2 uptake measured from the thermogravimetric analysis at ambient pressure. These results are close to those obtained by the calorimetry. The [CTA]Si–MCM-50 present the largest capacity of CO_2 adsorption 450 μmol g^{-1}, followed by the [CTA]Si–MCM-48 that adsorbed 360 μmol g^{-1}, while [CTA]Si–MCM-41, due to the limitations described previously, presented a reduced adsorption of 210 μmol g^{-1}.

3.3. Catalytic performances in transesterification of rapeseed oil with ethanol

Table 2 presents the results of transesterification of rapeseed oil with ethanol. Surprisingly, they disclosed that in spite of the pronounced strong basicity of ZrOCs in comparison with that of the hybrid materials; the oil conversion achieved in the presence of the hybrid materials is equivalent with [CTA]Si–MCM-41 and even higher with [CTA]Si–MCM-48 and [CTA]Si–MCM-50 to that measured on the ZrOCs in the same standard reaction conditions. In our standard conditions, the [CTA]Si–MCM-48 led to a vegetable oil conversion of 96% with a high selectivity for ethyl esters, 91%. By contrast, a conversion of 65% only was achieved with the ZrOCs sample. Among the basic hybrid catalysts, the following ranking was observed as regards their activity for rapeseed oil transesterification:

heat of ammonia adsorption but a reduced amounts of sites was probed on [CTA]Si–MCM-48, around 200 μ mol g^{-1}. The main difference among these two materials is the geometry of the silica arrangement; it can be concluded that the lamellar structure of [CTA]Si–MCM-50 allows a better exposition of the adsorption sites most likely located at the pore mouth; this might be limited in the cubic structure of the [CTA]Si–MCM-48.

The [CTA]Si–MCM-41 presents a hexagonal geometry with parallel one-dimensional pores. This material presents a lower cation/silica molar ratio (0), the half of the cation/silica ratio of the other materials (Table 1). This material is characterized by an initial heat

Table 2
Transesterification of rapeseed oil with ethanol (ethanolysis).

Catalyst	Conversion[a] (mol%)	Selectivity (mol%)[b]		
		Ethyl esters	Mono-glyceride	Di-glyceride
ZrOCs[c]	64	91	8.5	0.5
[CTA]Si–MCM-41	65	85	10	5
[CTA]Si–MCM-48	96	91	7	2
[CTA]Si–MCM-50	78	89	8	3
Blank	1.4	–	–	–

Reaction conditions: Temperature = 79 °C, alcohol/oil molar ratio = 18, catalyst mass = 2.5%, duration = 5 h.
[a] Oil conversion = sum of the molar yields in fatty acid esters, monoglycerides and diglyceride corrected by the amount of fatty chains.
[b] The molar selectivities are corrected by the amount of fatty chains.
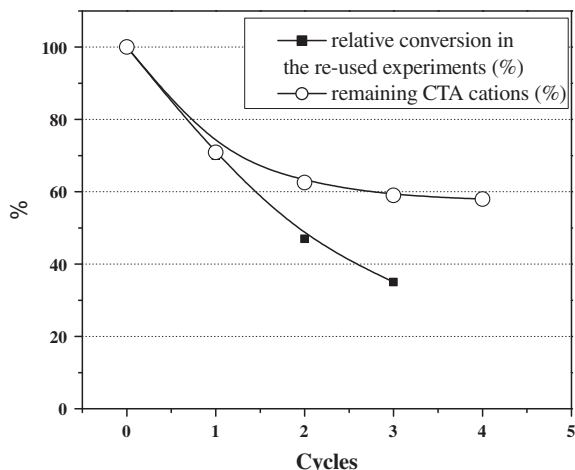[c] Pre-treatment: 1 h under vacuum at 400 °C.

Fig. 5. Re-usability of [CTA]Si–MCM-48: evolutions of the conversion and of the template content after successive cycles.

[CTA]Si—MCM-48 > [CTA]Si—MCM-50 > [CTA]Si—MCM-41

Within the hybrid material series, this ranking is in line with (1) total amount of sites probed by CO_2 adsorption and (2) the differential heat of CO_2 adsorption: the more energetic sites are also the most active.

Besides, the hybrid basic catalysts present the advantage of functioning without pre-treatment aimed at remove the physisorbed water and the more problematic carbonates species. However, the hybrid basic catalysts can only be used for running reactions at low temperature in contrast to the basic oxide, ZrOCs, characterized by a high thermal stability.

Finally, for the two types of materials, a peculiar attention was paid to evaluate the eventual contribution of homogeneous catalytic active species as follows: the solid bases were refluxed in ethanol for 5 h and then separated from the solid catalyst by hot filtration in order to perform a subsequent transesterification reaction with the recovered ethanol in the absence of added solid catalyst. The oil conversion achieved with the ethanol issued from ZrOCs extraction was close to that of the blank experiment [17]; for [CTA]Si–MCM-48, the conversion achieved represent less than 10% of that measured in the presence of the solid catalyst. In order to evaluate the recyclability of the hybrid material, the catalyst recovered after a first experiment was re-used for several cycles after an ethanol washing at ambient temperature. After each cycle, its template content was quantified by TGA. Fig. 5 shows the evolution of the conversion in the re-use experiments expressed as a relative conversion in regard to that of the fresh catalyst. The corresponding evolution of the template content was also presented. A stabilization of the template amount after the first cycle was observed while a continuous decrease in the activity occurred. This would indicate that initially the activity lost might be partly ascribed to the template extraction.

4. Conclusions

The as-synthesized hybrid catalysts of the M41S family, consisting of the template-containing molecular sieves, are highly ordered organic–inorganic materials. These catalysts present low specific areas, because their pores are occluded by the template. However, these templated molecular sieves exhibit a peculiar basicity ascribed to the presence of the ions pair: siloxi anion and the CTA$^+$ cation [14]. The hybrid catalysts were studied by microcalorimetry of CO_2 adsorption: they are characterized by a low heat of CO_2 adsorption (between 70 and 90 kJ mol^{-1}) and, interestingly, by

the complete reversibility of the adsorption at 30 °C. This level of differential heat of CO_2 adsorption is intermediate between the physisorption and the chemisorption. These hybrid catalysts were revealed as very efficient catalysts for the transesterification of rapeseed oils with ethanol at moderate temperatures (79 °C). An oil conversion of 96% was achieved in 5 h with the [CTA]Si–MCM-48 sample, the most active catalyst within the series.

We compared the hybrid materials with a more usual basic oxide, such as ZrOCs, which presents a strong basicity with heat of CO_2 adsorption of 130 kJ mol^{-1}. As expected for the most usual solid bases used in catalysis, the CO_2 adsorption is totally irreversible at 30 °C, which accounts for the formation of strongly CO_2 bonded species as carbonates. Contrary to our expectations, the catalytic performance of ZrOCs did not overreach that of the hybrid materials. On the contrary, its activity is only equivalent to that of the less active hybrid catalyst [CTA]Si–MCM-41 and was inferior to the activities of [CTA]Si–MCM-48, [CTA]Si–MCM-50. A priori, this ranking might result from the occurrence of too strong adsorptions of reactants and/or products on the surface of the strong inorganic base assuming that the fresh catalysts surface was only partially inhibited by the presence of stable carbonate species [17]. By contrast, one can assume that weaker adsorption of reactant and products would occur on the surface of the hybrid material, which might precludes a rapid and strong deactivation due to irreversible adsorption of reactants and/or products on the surface of the hybrid catalyst. Moreover, only a limited inhibition of the hybrid materials by atmospheric CO_2 is expected accounting for the weakness of the bonds between the superficial basic sites and the CO_2 species.

Therefore, these hybrids catalysts present the advantages to be easily synthesized and they do not need a previous activation due to their limited contamination by carbonatation. They catalyze efficiently basic demanding reactions tentatively explained by the occurrence, in the reaction media, of competitive adsorption highly favorable to the reactant molecules. This situation would compensate the presence of highly energetic basic sites that suffer presumably from the occurrence of strong adsorptions of reactants or products. However, if the inorganic strong bases may be regenerated via a thermal treatment, this cannot be applied in the case of the hybrid basic catalysts.

Acknowledgment

References

[1] F. Ma, M.A. Hanna, Bioresour. Technol. 70 (1999) 1–15.
[2] G. Vicente, M. Martínez, J. Aracil, Bioresour. Technol. 92 (2004) 297–305.
[3] A.F. Lee, K. Wilson, Top. Catal. 53 (2010) 11–12.
[4] C.Y. Chen, S.Q. Xiao, M.E. Davis, Micropor. Mater. 4 (1995) 1–20.
[5] J. Weitkamp, M. Hunger, U. Rymsa, Micropor. Mesopor. Mater. 48 (2001) 255.
[6] J.S. Beck, J.C. Vartuli, W.J. Roth, M.E. Leonowicz, C.T. Kresge, K.D. Schmitt, C.T.W. Chu, D.H. Olson, E.W. Sheppard, S.B. McCullen, J.B. Higgins, J.L. Schlenker, JACS 114 (1992) 10834.
[7] H. Van Bekkum, E.M. Flanigen, P.A. Jacobs, J.C. Jansen, Introduction to Zeolite Science and Practice, Elsevier, 2001.
[8] C.M. Yang, K.J. Chao, J. Chin. Chem. Soc. 49 (2002) 883.
[9] F. Fajula, D. Brunel, Micropor. Mesopor. Mater. 48 (2001) 119.
[10] M.H. Valkenberg, W.F. Hoelderich, Catal. Rev. 44 (2002) 321.
[11] C.N. Pérez, E. Moreno, C.A. Henriques, S. Valange, Z. Gabelica, J.L.F. Monteiro, Micropor. Mesopor. Mater. 41 (2000) 137.
[12] Y. Kubota, Y. Nishizaki, H. Ikeya, M. Saeki, T. Hida, S. Kawazu, M. Yoshida, H. Fujii, Y. Sugi, Micropor. Mesopor. Mater. 70 (2004) 135.
[13] Y. Kubota, Y. Sugi, T. Tatsumi, Catal. Surv. Asia 11 (2007) 158–170.
[14] L. Martins, T.J. Bonagamba, E.R. Azevedo, P. Bargiela, D. Cardoso, Appl. Catal. A: Gen. 312 (2006) 77–85.
[15] L. Martins, D. Cardoso, Micropor. Mesopor. Mater. 106 (2007) 8–16.

[16] A.C. Oliveira, L. Martins, D. Cardoso, Micropor. Mesopor. Mater. 120 (2009) 206–213.
[17] B. Hamad, A. Perard, F. Figueras, F. Rataboul, S. Prakash, N. Essayem, J. Catal. 269 (2010) 1–4.
[18] C.F. Cheng, D.H. Park, J. Klinowski, J. Chem. Soc. Faraday Trans. 93 (1997) 193.
[19] A.M. Doyle, E. Ahmed, B.K. Hodnett, Catal. Today 116 (2006) 50–55.
[20] N. Essayem, V. Martin, A. Riondel, J.C. Védrine, Appl. Catal. A: Gen. 326 (2007) 74.
[21] S. Brunauer, P.H. Emmet, E. Teller, JACS 60 (1938) 309.
[22] B. Hamad, R.O. Lopes de Souza, G. Sapaly, M.G. Carneiro Rocha, P.G. Pries de Oliveira, W.A. Gonzalez, E. Andrade Sales, N. Essayem, Catal. Commun. 10 (2008) 92.